ORIGINAL ARTICLE

Rotated clinching process for two-layer metallic sheets

Yulin He[1] · Lianfa Yang[1] · Pengju Zong[1] · Jing Dang[1] · Jianping Ma[1]

Abstract

Mechanical clinching is a process of joining various sheets using a punch and a die and has been widely applied in automobile manufacturing. A rotated clinching process using two rotated heads and a flat-bottomed fixed die was proposed in this study. An experimental device was developed and rotated clinching experiments were conducted on 1.5-mm-thick Al1060 sheets using this approach. Shear and pull-out tests of the joints with various vertical reductions of rotated heads were conducted to evaluate the static joining strength. The failure modes of joints and the geometric characterisation of the joint profile in terms of interlock and neck thickness were analysed. Preliminary test results show that the joint strength exhibited evident directionality, where the force applied in the transverse direction was the largest. The maximum strength was 40% that of the Al1060 sheet. Full tearing failure and partial tearing with unbuttoning failure were the main joint failure modes. With increasing vertical reduction of the rotated heads, the neck thickness changed less and the interlock increased, reaching 33.3% of the lower sheet thickness.

Keywords Aluminium sheet · Rotated clinching process · Joining strength · Failure mode

1 Introduction

In recent years, with the improvements in the economy and environmental protection requirements, lightweight technology has developed rapidly. Various lightweight materials, particularly aluminium and its alloys, which have unique properties in terms of appearance, light weight, formability, specific strength, and corrosion resistance [1], have been used in diverse applications. Resistance spot welding is not suitable for joining different materials owing to their dissimilar heat capacities and melting temperatures, which would cause intermetallic compounds, brittle phases, electrochemical corrosion, thermal deformation, and stress concentration around the interface between different metals [2], affecting the joint strength. Mechanical connection technology, such as self-piercing riveting and mechanical clinching, can effectively prevent these problems without introducing heat into the sheets to be joined. In self-piercing

riveting, two or more sheets are joined by directly piercing the sheets with a rivet, which increases the product weight and introduces cost issues [3]. In mechanical clinching, two or more sheets are locally plastically deformed to produce an interlock using a punch and die. Mechanical clinching does not require the use of subsidiary elements such as rivets or screws, enabling significant cost reduction and eliminating any special preparation of the sheet surfaces [4]; thus, it can easily be automated and provide rapid joining. With these advantages, mechanical clinching has attracted increasing attention in many manufacturing processes involving joining of the same or dissimilar sheets such as steels and aluminium alloys, copper, magnesium, titanium alloys, and polymers.

In conventional mechanical clinching, the joint strength is mainly determined by the final joint geometry, including characteristics such as the neck thickness and interlock, which in turn depends on the tool geometry (i.e. that of the punch and die). In recent research, two main types of tools have commonly been used in mechanical clinching: round and rectangular tools. A round tool can only deform a material, whereas a square tool can deform and cut the material.

Round tools include fixed groove dies, split dies, and flat dies. Extensive research has been focused on the use

✉ Lianfa Yang
  y-lianfa@163.com

[1] Faculty of Mechanical and Electrical Engineering, Guilin University of Electronic Technology, GUIDIAN Jinjiling Campus, BOX: 19-04 1 Jinji Road, Qixingqu 541004 Guilin, China

of round tools in mechanical clinching. In terms of studies on fixed groove dies, Hamel et al. [5] investigated mechanical clinching forming for steel with respect to the process parameters using the finite element method. The results showed that an increase in die depth resulted in an increase in interlock. Paula et al. [6] studied the effects of different die geometries on both the neck thickness and interlocking of joints for Al1100 using the finite element method. Their results demonstrated that the die diameter and groove thickness, shape, and depth did not benefit the joint interlock and could cause neck thickness problems. Oudjene and Ben-Ayed [7] investigated the effects of tool geometry on the clinch joint strength of aluminium alloy Al5754 as well as on its shape (neck thickness and interlock) using the Taguchi method. Their experimental results showed that the clinch joint strength was highly dependent on the tool geometry, particularly the die diameter parameters. Lee et al. [8] examined the effects of die radius, depth, and groove shape on the joint characteristics of advanced high strength steel DP780 and Al5052 alloy sheets using finite element analysis. They concluded that the interlock length and neck thickness could determine the joining strength. Mucha [9] investigated the effects of the geometrical parameters of the die on the joint interlock size of advanced high strength steel by performing finite element analysis and experimental tests and found that the die impression geometry, particularly that of the groove, considerably influenced the interlock and neck thickness. Kim et al. [10] evaluated the effects of the shape parameters of the tools on the joining strength and optimised clinching tools using the design experiments method and finite element analysis. The results showed that optimising the shape parameters improved the joining strength. Coppieters et al. [11] studied the process-induced bottom defects in joining two layers EN AW-6082 T6 sheets with limited ductility by performing a finite element simulation. Four ductile damage models are used to predict the occurrence of bottom cracks. The analysis results showed that the bottom cracks had no adverse effects on the static and fatigue strength of the joints [11]. Brzezin'ski et al. [12] investigated the effects of the die shape on the material flow in sheet combination, including an ultra-high strength steel sheet with limited ductility, by performing a finite element simulation and experimental tests. To increase the interlock between the ultra-high strength steel sheets, Abe et al. modified the bottom angle of the die groove, the die depth was decreased, and the groove in the die was eliminated to join high strength steel and aluminium alloy sheets [13]. In contrast to a fixed groove die, a hole clinching process using a fixed die with a flat bottom was developed [14]. This process can provide a larger interlock, although the lower sheet requires a prepunch. Neugebauer et al. [15] proposed a dieless clinching process with a

punch and flat die (flat anvil). The results revealed that the larger the punch diameter, the larger the neck thickness. In this process, the movement and force of the punch must be controlled to control the flow of materials. A new flat clinching process was developed at Chemnitz University of Technology [16]. This process can effectively control material flow by employing a punch, special blank holder, and flat die. Atia and Jain [17] investigated material flow with various blank holder designs and the effects on interlocking. Wood and aluminium [18], two-layer aluminium alloy Al5052 sheets [19], and three-layer sheets (two-layer Al1060 sheets and one-layer steel sheet) using two interlocks to create a thin-walled structure [20] were joined via this flat clinching process. By optimising the blank holder design, the interlock was improved; however, a high blank holder and forming forces were required in this process. An increase in blank holder force induces a decrease in interlock and an increase in neck thickness. Therefore, the die should be designed to produce a high interlock (between the sheets) without excessively reducing the neck thickness of the upper sheet. He and Huang [21] developed a split die composed of a cone die anvil and two divisible die parts. When the sheets are joined in this approach, the divisible die parts are closed to form an inverted conical die cavity that is similar to a fixed die. The sheet components can be removed from the open die after the process is completed. A reasonable cone angle and die depth can provide a larger interlock. Further, Lambiase and Di Ilio [22] first presented another split die, an extensible die, which is composed of a series of moveable segments, die with a flat anvil, fixed die, and rubber spring. Mechanical clinching in low carbon steel AISI 1005 sheets [23], aluminium alloy Al5754 [24], aluminium alloy Al5052 [25], and titanium sheet materials [26] were studied experimentally using extensible dies with three moveable segments. The results showed that larger interlocks were produced when extensible dies were used than when fixed groove dies were used. Witkowski [27] studied the effects of using different extensible dies with two, three, and four moveable segments on the joint
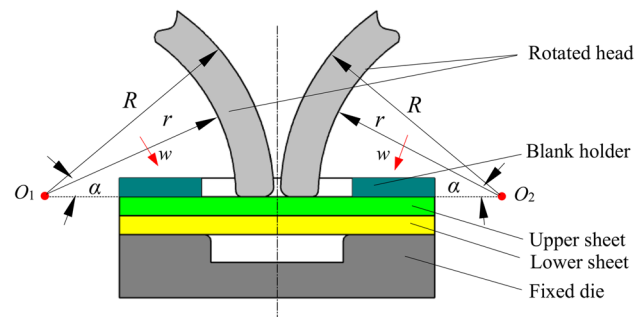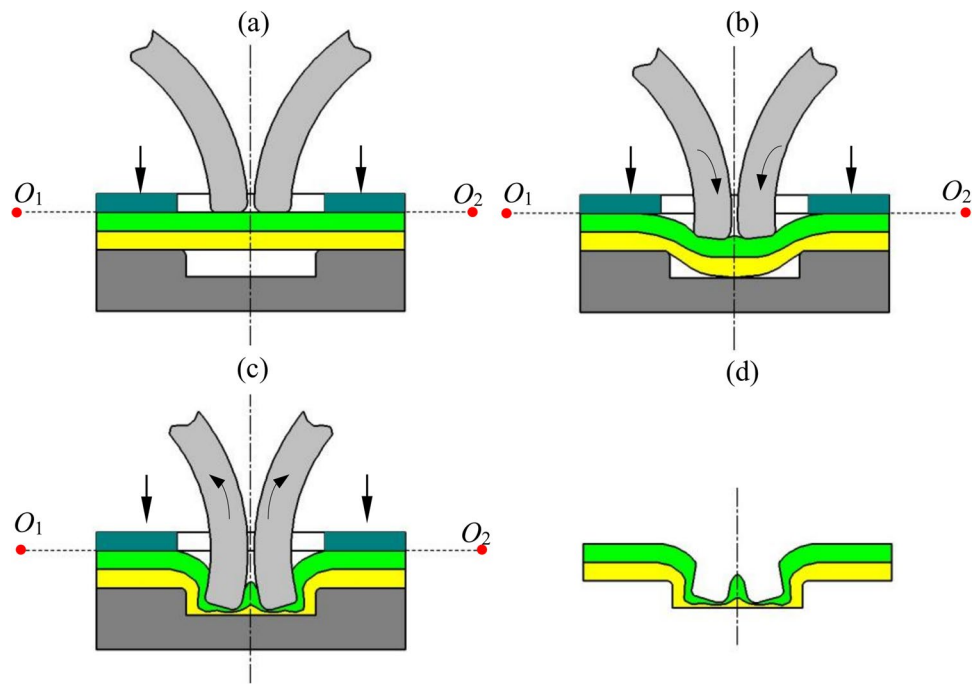

Fig. 1 Schematic of rotated clinching

Fig. 2 Process sequence of rotated clinching: **a** initial positions; **b** localised plastic deformation of the upper and lower sheets; **c** interlock formation and retraction; **d** the joint obtained by rotated clinching

strength by experimental analysis. The results showed that the number of moveable segments did not significantly affect the joint strength and that the interlock shape was not axially symmetrical.

In terms of rectangular tools, Mucha [28] investigated rectangular clinched joint behaviour for various load directions by performing experimental analysis. Varis [29] compared fixed groove and extendible dies with round and rectangular punch clinching for high strength structural steel. If the thicker material was placed on the die side or the total thickness of the joined sheets was 4.0 mm, a square shaped joint could bear a higher shear load than a round one. Zhao et al. [30] studied the clinched joints of 5052 aluminium alloy sheets with extendible and rectangular dies. The results showed that the minimum neck thickness of the rectangular joints was lower than that of the round joints and that the corresponding interlock was larger. The strength of the rectangular joints was 1.7 times that of the round ones. Lambiase [31] investigated the mechanical behaviour of polymer–metal hybrid clinched joints with fixed groove dies, split dies, flat dies, and rectangular tools. The results showed that the joining forces were low and the peeling performance was high with rectangular tools.

As previously stated, in a mechanical process using a fixed die, a fixed die with a groove is complicated, and as

the displacement of the punch increases, the upper sheet becomes quite thin near the punch corner. In mechanical processes using split dies that can improve interlock, the die structure is more complicated. To address these shortcomings, this study proposes a rotated clinching process. In this approach, the punch is replaced with two rotated heads which are arc structures of the same shape and size, and the die is a fixed die with a square flat bottom. In contrast to the movement of the punch, which rotates vertically around the axis, in rotated clinching, the heads rotate horizontally around two contrariwise shafts and demould by reverse rotation. The interlock can be increased by rotating these heads. The objective of this work was to verify experimentally the feasibility of the rotated clinching process for joining sheet metals. The schematic of proposed rotated clinching process is described in Sect. 2. An experimental device for rotated clinching was designed and developed by the authors, and preliminary experiments were conducted on 1.5-mm-thick Al1060 sheets by rotated clinching under different rotated vertical reductions, and shear and tensile strength tests were conducted on the joints to evaluate the static joining strength, and this is reported in Sect. 3. Subsequently, the static joining strength, failure modes, and geometric characteristics of the cross-sectional profiles of joints in terms of interlock and neck thickness are analysed in Sect. 4. The conclusions and recommendations are presented in Sect. 5.

Table 1 Chemical composition of Al1060

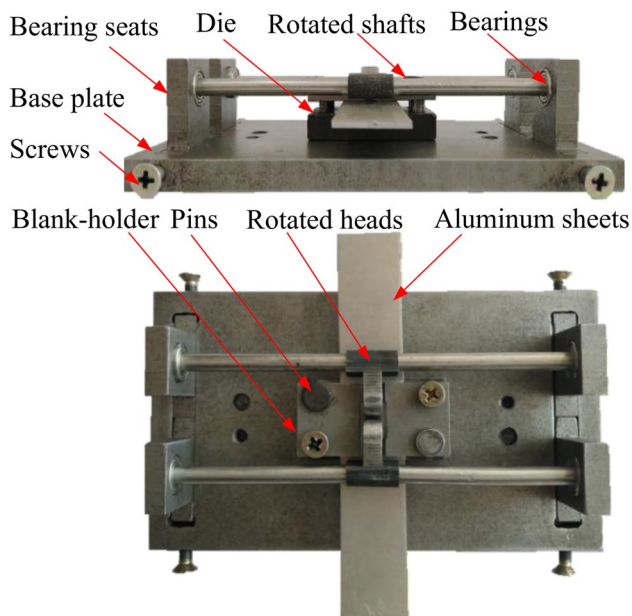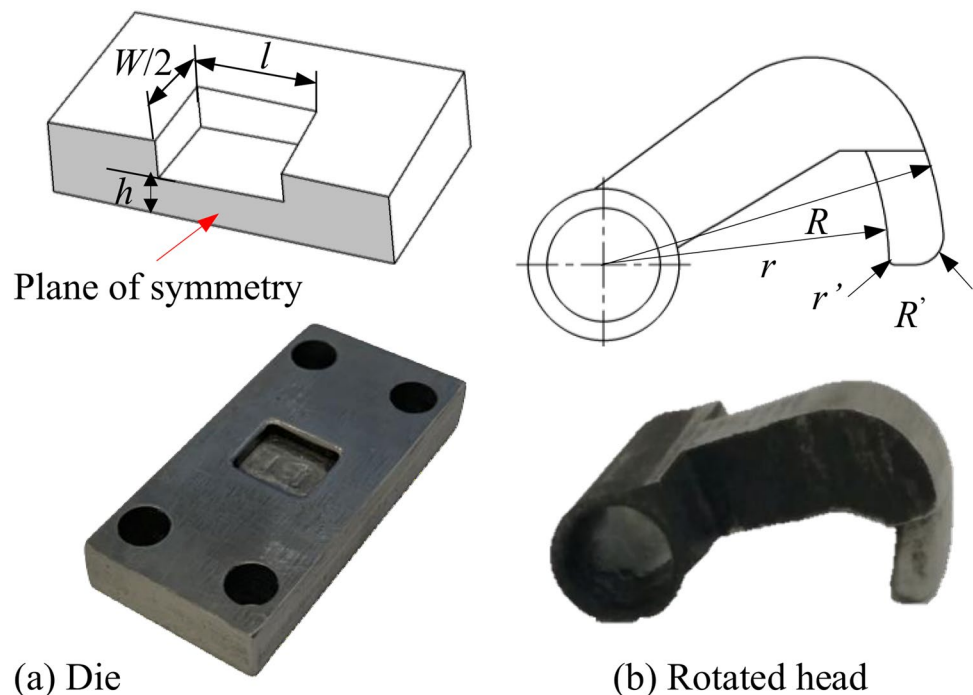|	Si (wt%)	Fe (wt%)	Cu (wt%)	Mn (wt%)	Zn (wt%)	Al (wt%)
Al1060	0.43	0.33	0.16	0.038	0.01	99.032

Fig. 3 Rotated clinching experiment device

2 Rotated clinching process

The principle of the rotated clinching process is shown in Fig. 1. Two overlapped metal sheets are clamped against the fixed die with a square flat bottom by a blank holder. Two rotated heads rotate simultaneously downwards towards the fixed die around their centres of rotation (O_1 and O_2) at a pre-set angular velocity w. The rotated heads are arc structures of radius r and R are mounted on contrariwise rotating shafts

and exert pressing forces on the sheets to draw the materials into the die cavity to cause plastic deformation. The sheet materials spread out in the die cavity upon pressing due to the rotating movement of the heads. When the pre-set rotation angle α is reached, the rotated heads stop their downwards rotation and rotate upwards to retract. The result is a non-axisymmetric mechanical joint created between the rotated heads and die side. Figure 2 illustrates the forming process.

## 3 Experimental procedures

3.1 Materials

Thin rolled sheets of Al1060 with nominal thickness $t = 1.5$ mm were used as the base materials for this study. Table 1 lists the elemental compositions. The mechanical properties of the Al1060 sheet were measured by uniaxial tensile testing (WDW-100GD testing machine). According to the test results, the elastic modulus of Al1060 is 54.5 GPa, its Poisson's ratio is 0.33, its tensile strength is 112 MPa, and the average value of its maximum tensile force is 2690 N. The samples used for the rotated clinching experiments were cut into rectangular strips (length 80 mm × width 20 mm) from a unique sheet.

3.2 Experimental device

Figure 3 shows the rotated clinching device designed and developed by the authors. This device comprises two rotated heads, a fixed die with a square flat bottom, two

Fig. 4 Dimensions and photos of tools using for rotated clinching

(a) Die   (b) Rotated head

Fig. 5 The finite element simulation of rotated clinching: **a** finite element model; **b** the final joint obtained by rotated clinching through finite element simulation

(a)

(b)
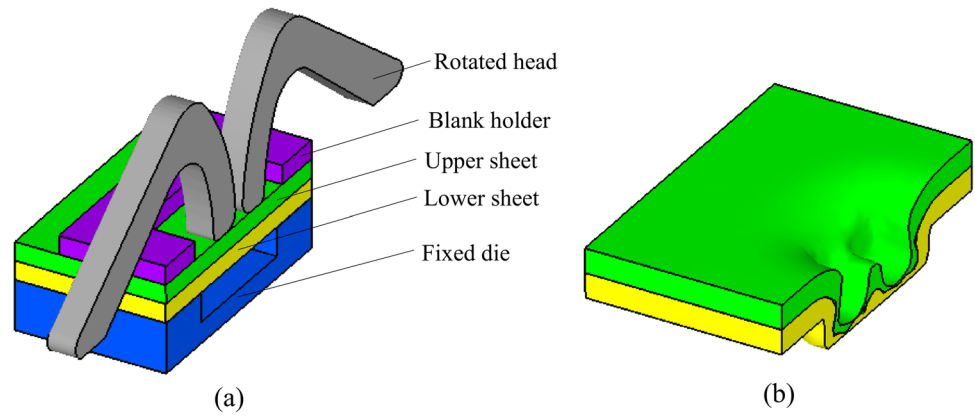
rotated shafts, a blank holder, base plate, bearing seats, positioning pins, and bolts. The rotated heads are mounted on the rotated shafts, and the rotated shafts are installed on the bearing seats through the bearings. The positioning pins are fixed on the base plate to locate and guide the blank holder and die. During the forming process, the structural parameters of the tools with the rotated heads and die are important factors that affect the joint formation. Figure 4 shows the dimensions of the rotated clinching tools. To obtain the defined design parameters of the rotated clinching tools, the finite element model of rotated clinching is developed, as shown in Fig. 5. The forming process using different parameters is simulated, and various joints are obtained. The main parameters of the tool with better joints are preliminarily determined in

this study, that is, $l = 10.5$ mm, $W = 9$ mm, $h = 2.3$ mm, $R = 18$ mm, $r = 15$ mm, $R' = 1.5$ mm and $r' = 0.3$ mm.

3.3 Rotated clinching experiments

The rotated clinching experiments were conducted using a microcomputer controlled electronic universal testing machine (WDW-100GD) with 100 kN full scale force at a constant pressure head speed of 30 mm/min, as shown in Fig. 6a.

As shown in Fig. 7, pressure P was applied to the rotated heads by the pressure head during the experiments to rotate them around the shafts. α directly affects the joint formation. When α reaches a specified value, the pressure heads stop moving down, vertical reduction of the rotated heads

Fig. 6 Experimental procedures for rotated clinching and strength tests of joints: **a** rotated clinching experiment; **b** shear and pull-out test
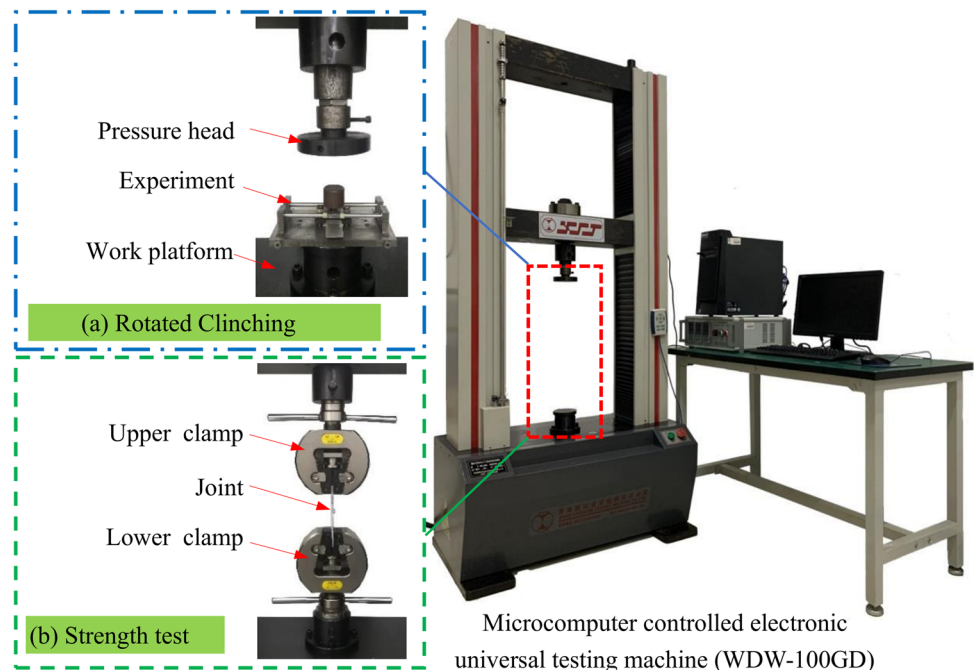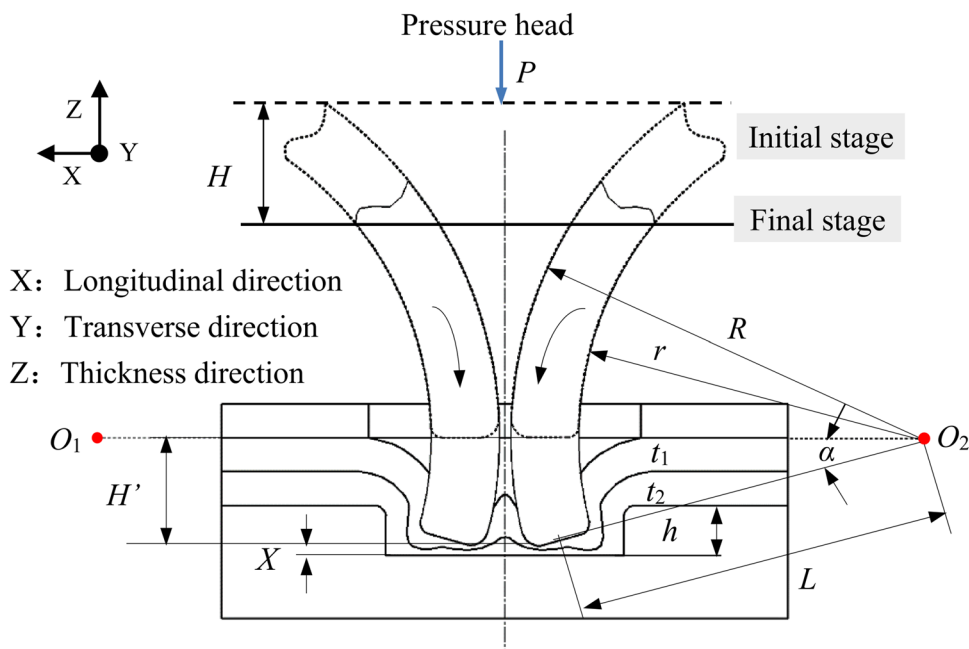

Microcomputer controlled electronic universal testing machine (WDW-100GD)

Fig. 7 Main geometric parameters of the joint produced by rotated clinching

is H', displacement of the pressure head is H, and distance between the centre of the rotated shaft (O_2) and the position of minimum bottom thickness is L. $H = H'$ and $L \approx 1/2(R + r)$ were assumed during the experiment, and the relationship between these parameters can be expressed as follows:

$$H = H = 1/2(R + r) \cdot \sin \alpha = t_1 + t_2 + h - X_{min} \quad (1)$$

where h is the die depth; t_1 and t_2 are the thicknesses of the upper and lower sheets, respectively; and X_{min} is the minimum bottom thickness. In the present study, $t_1 = t_2 = 1.5$ mm. During the clinching forming process, it is necessary to ensure that the sheet material can form an interlock and cannot be crushed. According to the theoretical calculation and simulation analysis results based on the tool dimensions, the range of α that could produce interlock was obtained. Further, H was derived from Eq. (1) and was determined to range from 4 to 4.6 mm. To study the effects of various H' of the rotated heads on the joints, H was set to 4.1, 4.2, 4.3, 4.4, 4.5, and 4.6 mm to control α. Figure 8 shows the partial joints with different reductions of the rotated heads produced by the rotated clinching experiment.

3.4 Shear test

Single lap shear tests with different rotated head reductions were conducted to obtain the connection capacity in the horizontal direction of the clinched joints produced by rotated clinching. Considering the joint shape, there were two forces applied in the single lap shear test; in particular, the force was applied in the transverse or longitudinal direction. As shown in Fig. 7, the transverse and longitudinal directions (Y and X directions) are the length and width directions of the joint, respectively. Figure 9a and b show the specimens used in the single lap shear test. Two spacers with lengths of 20 mm × 20 mm were employed to concentrate the load for all configurations during the single lap shear test. The spacer thickness was 1.5 mm.

The single lap shear tests were conducted using a microcomputer controlled electronic universal testing machine (WDW-100GD) with 100 kN full scale loads at a constant crosshead speed of 2 mm/min until complete

Fig. 8 Surfaces on the **a** rotated head side and **b** die side of partial joints produced by rotated clinching
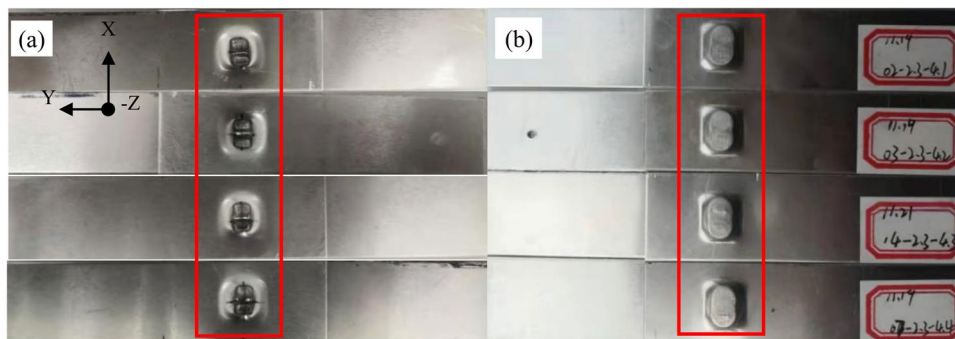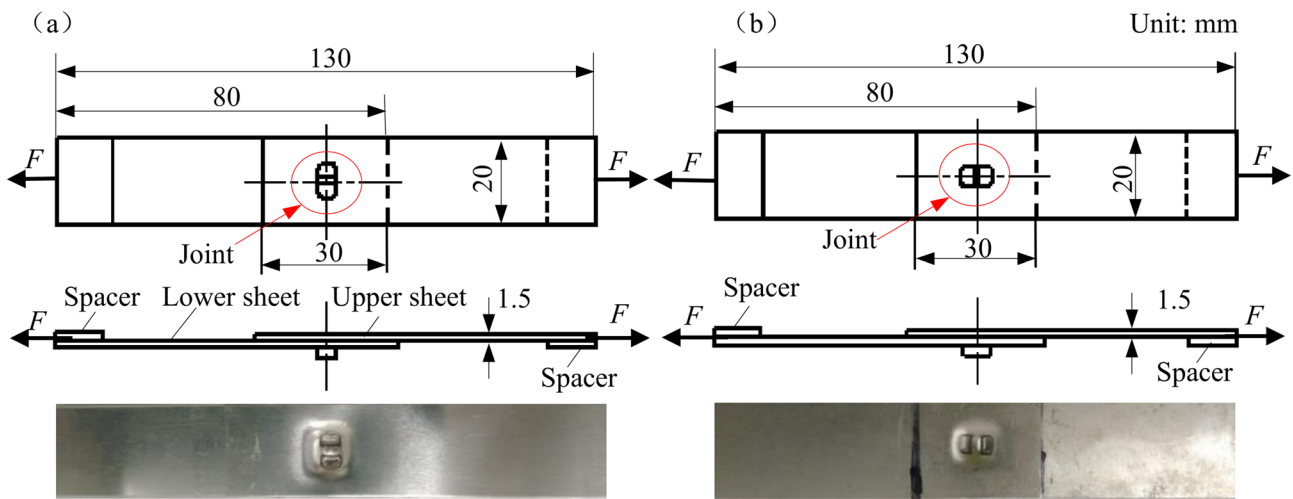
Fig. 9 Configuration and boundary conditions when the force was applied to the specimen in the **a** transverse and **b** longitudinal directions in the single lap shear test

separation of the sheets, as shown in Fig. 6b. For each processing condition, three specimens were tested, and the maximum of the force–displacement curve was analysed in each test.

Fig. 10 Specimen used in the tensile test: **a** dimensions and **b** photograph

3.5 Pull-out test

Pull-out tests with different vertical reductions of the rotated heads were conducted to evaluate the joint resistance to pull-out loading vertically in the thickness direction (Z direction shown in Fig. 7) of the clinched joints produced by rotated clinching. The joined sheets were fully separated by loading in the thickness direction. An H type specimen was used in the pull-out tests, and Fig. 10 shows the configuration and boundary conditions of the specimen. The test process was the same as that in the single lap shear test.
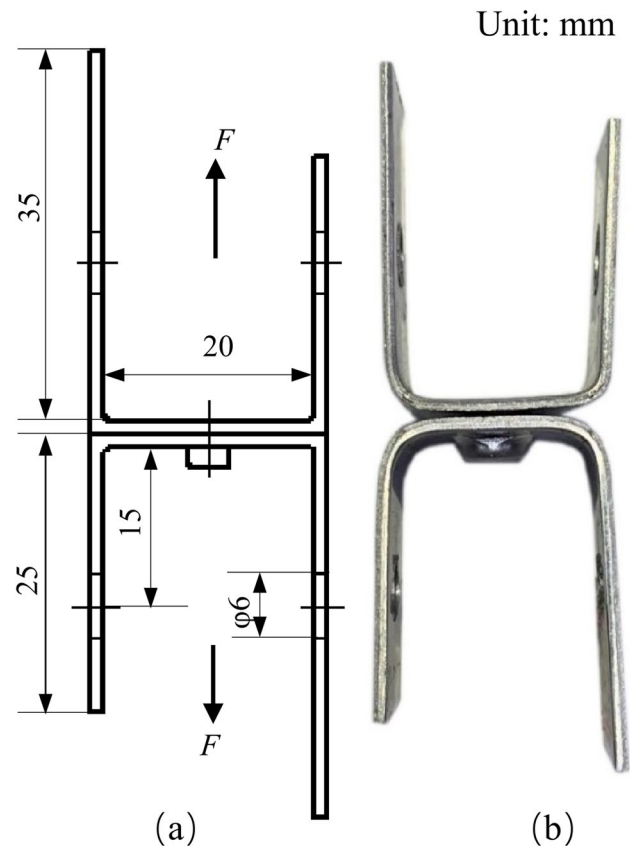
4 Results and discussion

4.1 Joining strength

The static joining strength of rotated clinching is represented by the shear and pull-out strengths. Shear strength

Table 2 Average maximum forces loaded on joints with various vertical reductions of the rotated heads in the strength tests in different directions and maximum forming force in rotated clinching for Al1060 sheets

H (mm)	F_{TS} (N)	F_{LS} (N)	F_P (N)	F (kN)
4.1	739	310	330	18.7
4.2	753	326	383	19.9
4.3	764	328	401	21.7
4.4	917	324	430	23.2
4.5	997	343	437	25.4
4.6	941	311	503	27.2

refers to the maximum force measured during shear testing, including the maximum shear forces in the transverse direction (i.e. transverse force F_{TS}) and in the longitudinal direction (i.e. longitudinal force F_{LS}). Pull-out strength refers to the maximum pull-out force measured in the thickness direction (i.e. pull-out force F_P). Because the joining strength of the joint is expressed by force in Newtons, whereas the tensile strength of the base material Al1060 is in Megapascals, for the convenience of comparison, both strengths are used in Newtons. In this study, the strength of the base material Al1060 refers to the average value of the maximum tensile force in the uniaxial tensile test, and its value is 2690 N.

To analyse the static joining strengths of the joints with different vertical reductions of the rotated heads for Al1060 sheets, Table 2 summarises the average maximum F_{TS}, average maximum F_{LS}, and average maximum F_p for the three test specimens for each processing condition in the strength test as well as the maximum forming force F on the joints during rotated clinching. F_{TS} is the largest, at 2.3–3 times F_{LS} and 1.9–2.3 times F_p. In addition, the maximum F increases as the vertical reduction of the rotated heads increases, reaching 27.3 kN when $H = 4.6$ mm.

The force and displacement curves show the maximum shear and pull-out force, and Fig. 11 presents the maximum values of the three test specimens for each vertical reduction of the rotated heads. In the shear test in transverse direction, when $H = 4.5$ mm, the maximum F_{TS} of the joint reaches 1090 N, as shown in Fig. 11a, which is approximately 40% that of the base material Al1060. Meanwhile, in the shear test in longitudinal direction, when $H = 4.3$ mm, the maximum F_{LS} of the joint reaches 388 N, as shown in Fig. 11b, which is approximately 14.4% that of Al1060. In the pull-out strength in the thickness direction, when $H = 4.6$ mm, the maximum F_P of the joint reaches 623 N, as shown in Fig. 11c, which is approximately 23% that of Al1060.

As demonstrated above, the joining strength of the joints created by rotated clinching exhibits clear directionality. This property should be properly considered when joining metal sheets. Figure 11 also shows that in the strength tests, when the force on the joint is maximum, its displacement is not maximum. These properties may be related to the failure mode and geometrical shape of the joint.

4.2 Failure modes

As can be seen from Fig. 11, the force–displacement curves under different conditions vary in the strength tests, and the failure modes of the specimens may be different. Among all specimens with different reductions of the rotated heads used in the single lap shear and pull-out tests, there were four failure modes: full tearing, partial tearing with unbuttoning, partial shearing with unbuttoning, and full unbuttoning.
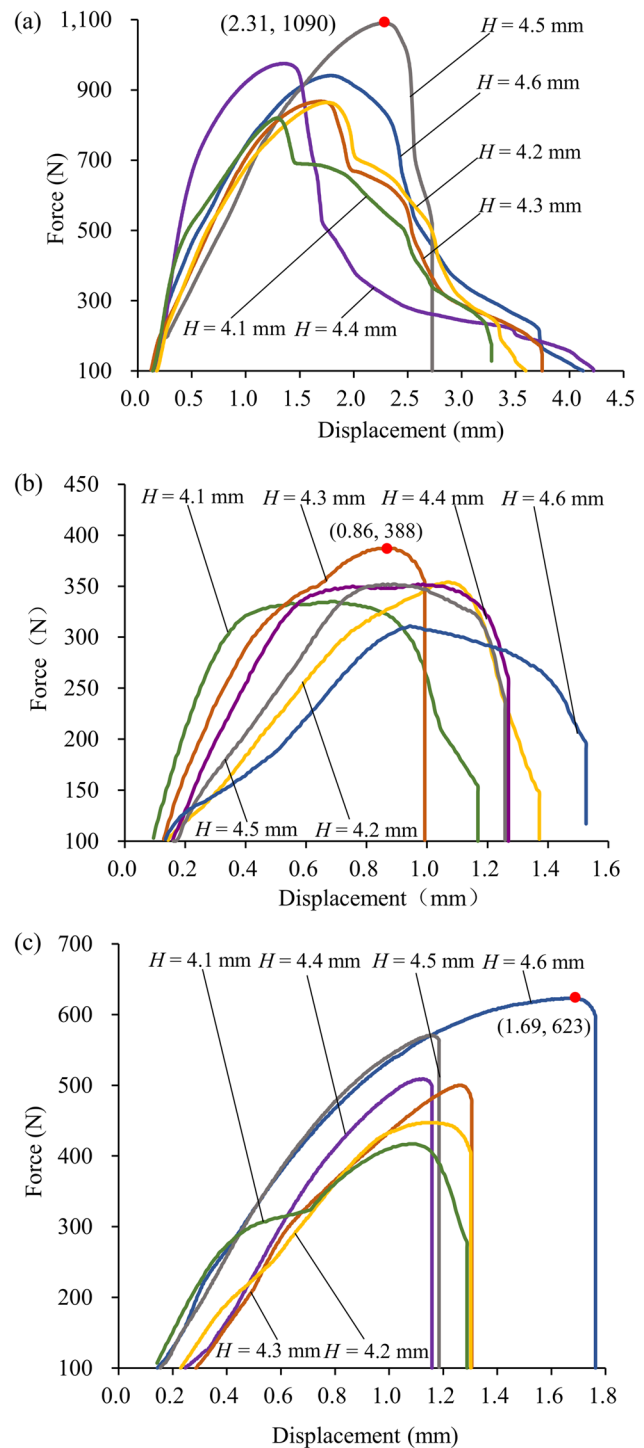

Fig. 11 Force and displacement curves of joints with different reductions of the rotated heads in various strength tests: **a** shear test in transverse direction; **b** shear test in longitudinal direction; **c** tensile test in the thickness direction

Figures 12, 13, and 14 depict the failure modes of the specimens. As can be observed from Fig. 12, in the single lap shear tests in transverse direction, there are three failure

Fig. 12 Failure modes of specimens in the single lap shear tests in transverse direction: **a** partial tearing with unbuttoning, **b** full tearing, and **c** full unbuttoning failure modes
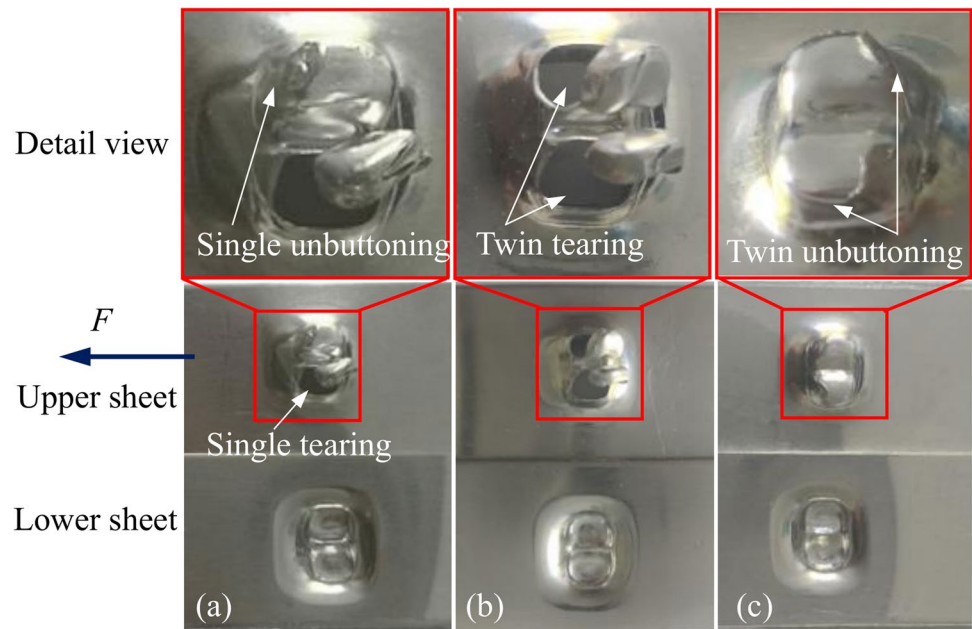
modes: full tearing, partial tearing with unbuttoning, and full unbuttoning. Here, the full tearing failure mode is prevalent, constituting approximately 76.5% of the failures. In the single lap shear tests in longitudinal direction, there are two failure modes: partial tearing with unbuttoning and partial shearing with unbuttoning, as shown in Fig. 13, where the unbuttoning with tearing failure mode is prevalent, corresponding to approximately 61.1% of the failures. In the pull-out tests in the thickness direction, there are two failure modes: full unbuttoning and partial tearing with unbuttoning, as shown in Fig. 14, where unbuttoning with tearing is the main failure mode, accounting for approximately 81.3% of the failures.

Twin tearing, single tearing, single shearing, and twin buttoning failures are referred to as full tearing, partial tearing with unbuttoning, partial shearing with unbuttoning,

and full unbuttoning failures, respectively (as shown in Figs. 12a, b, c and 13a, b, respectively). In full tearing, partial shearing with unbuttoning, and partial tearing with unbuttoning failures, when the force on the specimen increases to reach the yield strength of the Al1060 sheet, cracks begin to appear at the connection interface. Then, the material of the upper sheet is torn or sheared under further action of the force, and some part of the upper sheet remains in the lower sheet. Meanwhile, in full unbuttoning failure, the upper sheet material is completely separated from the lower sheet.

Table 3 summarises the main failure modes for all specimens with various vertical reductions of the rotated heads subjected to forces in different directions. The occurrence of one of these failure modes depends on the geometrical characteristics of the joint profile and local strength of the material.

Fig. 13 Failure modes of specimens in the single lap shear tests in longitudinal direction: **a** partial tearing with unbuttoning and **b** partial shearing with unbuttoning failure modes
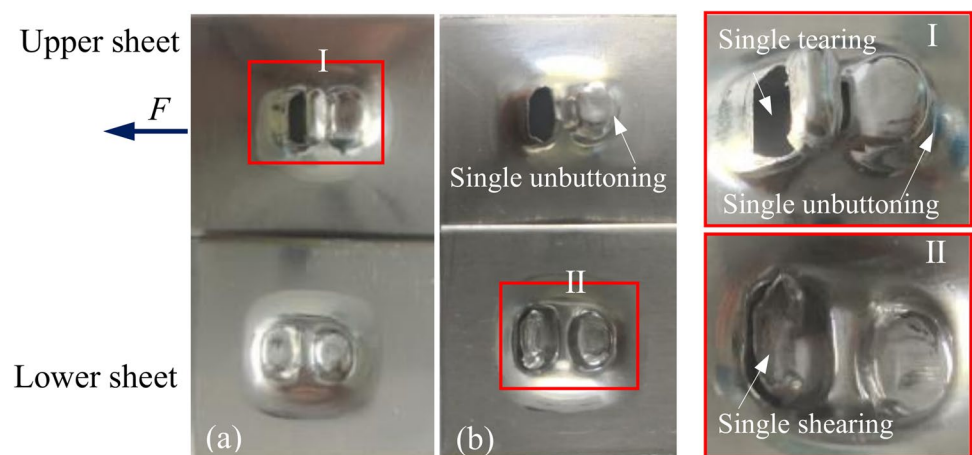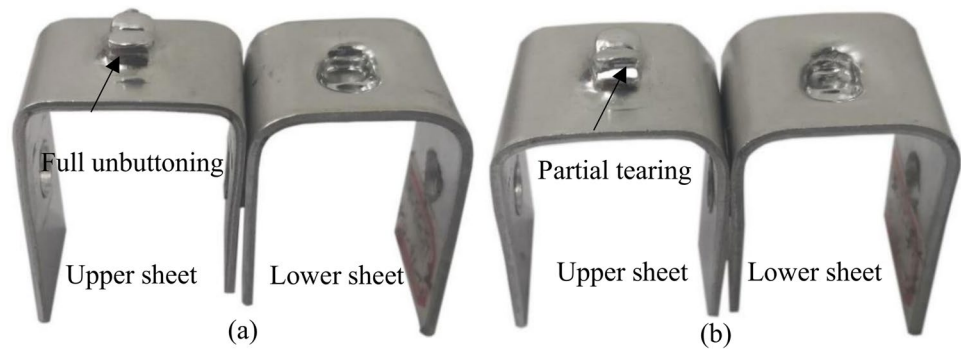
Fig. 14 Failure modes of specimens in the tensile tests in the thickness direction: **a** full unbuttoning and **b** partial tearing with unbuttoning failure modes

To analyse further the mechanical properties of the specimens with various vertical reductions of the rotated heads, Fig. 11a–c show the force–displacement curves of the specimens in the strength tests. The characteristics of the force as it increases to the peak for the specimens produced with various vertical reductions are almost the same, and the force increases gently before the peak, although there are differences between the force–displacement curves. A decrease in the force occurs after the force peak. However, different behaviours are observed in the joined samples because of the different failure modes in the shear and pull-out tests.

As shown in Fig. 11a, when the maximum force is reached, the joint fails by necking that results from early neck thinning. During neck thinning, a crack develops and propagates from the side of the joint near the applied force, causing the joint to be torn and thereby inducing a gradual decrease in the force. In this type of specimen, after the peak force is reached, the displacement increases as the cracks spread. Simultaneously, the interlock is gradually reduced until complete separation of the sheet occurs by tearing or shearing. Because of the different speeds of crack propagation, the length of displacement and the change in force vary in different reductions when subjected to transverse shear force.

Table 3 Main failure modes of joints with different force directions and various vertical reductions of the rotated heads

Vertical reduction H (mm)	Main failure mode in transverse direction	Main failure mode in longitudinal direction	Main failure mode in thickness direction
4.1	A	B	D
4.2	A	B	B
4.3	A	B	B
4.4	A	C	B
4.5	A	C	B
4.6	A	C	B

A full tearing, *B* partial tearing with unbuttoning, *C* partial shearing with unbuttoning, *D* full unbuttoning

For the specimens in the shear test in longitudinal direction, joint failure occurred after the peak force was reached due to partial necking that resulted from early neck thinning, as shown in Fig. 11b, and then the joint separated via unbuttoning with tearing. During neck thinning, a crack develops and propagates from the side of the joint near the applied force, causing the force to decrease gradually. Meanwhile, on the side of the joint away from the applied force, the mechanical interlock is reduced to almost zero, causing sudden separation of the sheet by unbuttoning, and then the force decreases immediately.

The specimens in the pull-out test in the thickness direction failed via tearing with unbuttoning. Therefore, after the peak, the pull-out force decreased almost immediately because of the sudden separation of the sheet, as shown in Fig. 11c. At $H = 4.1$ mm, the samples failed by full unbuttoning, which is different from the other force curves.

With the same vertical reduction of the rotated heads, the mechanical properties of the specimens undergoing full tearing failure in the shear test in the transverse direction are better than those of the other specimens.

4.3 Cross-sectional profiles

To analyse the different mechanical properties of joints produced with various vertical reductions of the rotated heads, the joints produced by rotated clinching were sectioned in the longitudinal direction, and the cross-sectional profiles of the clinched joints were measured using an optical microscope (model PAIRSEN 1000 M). The main geometrical parameters, such as neck thickness Δt, interlock Δs, and minimum bottom thickness X_{min} of the clinched joints, were measured using a Vernier calliper.

Figure 15 presents the cross-sectional profiles of clinched joints with different vertical reductions of the rotated heads, as well as the main characteristic parameters. Asymmetries can be observed in the cross-sectional profiles of the actual joints. The maximum and minimum Δt and Δs as well as

Fig. 15 Cross sections and main characteristic parameters of joints with different vertical reductions H: X, longitudinal direction; Y, transverse direction; Z, thickness direction; Δt, thickness; Δs, interlock; X_{min}, minimum bottom thickness
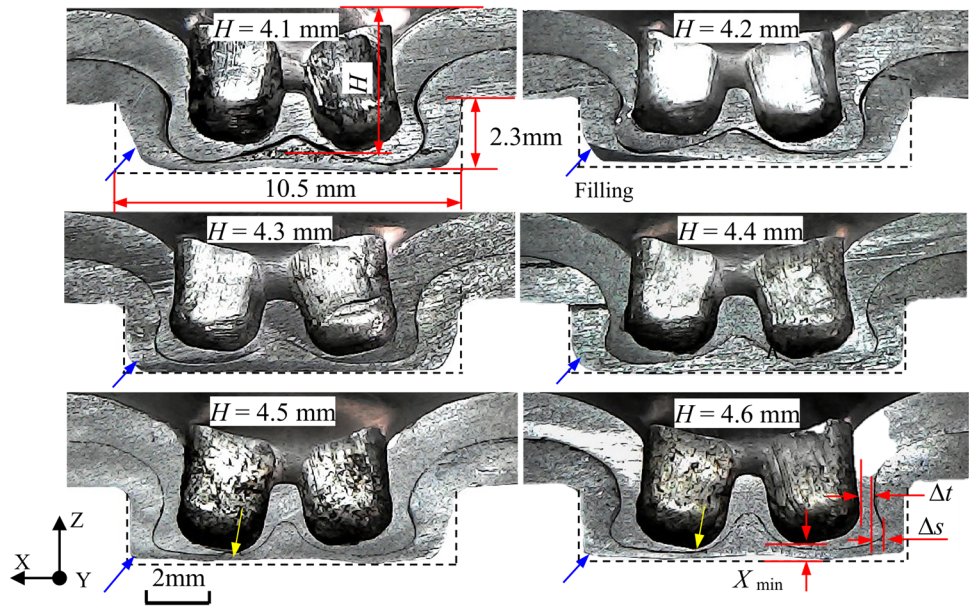
X_{min} were measured, and Fig. 16 shows the values of these parameters.

As can be seen from Figs. 15 and 16, with increasing H (i.e. increasing α) of the rotated heads, the interlock between the sheets becomes more significant. The maximum Δs is 0.5 mm when $H = 4.6$ mm and X_{min} is low, whereas the maximum and minimum Δt values are relatively stable, and the mean Δt value is almost constant. In addition, the filling of the material improves with increasing H, as indicated by the blue arrows in Fig. 15, whereas the die groove is not completely filled when H is small. When $H = 4.4$ mm, the symmetry of joint and filling uniformity of the material are better. However, the bottom thinning of the upper sheet close to the external chamfer R' of the rotating head is evident (as indicated by the yellow arrows in Fig. 15), which is also the reason for the different failure modes of the joints.

Fig. 16 Δt, Δs, and X_{min} for joints with different vertical reductions

H	Δt_{min}	Δt_{max}	Δt_{mean}	Δs_{min}	Δs_{max}	Δs_{mean}	X_{min}
4.1	0.35	0.40	0.380	0.15	0.26	0.205	0.72
4.2	0.34	0.42	0.380	0.20	0.26	0.230	0.64
4.3	0.35	0.42	0.385	0.22	0.30	0.260	0.62
4.4	0.38	0.40	0.390	0.30	0.32	0.310	0.54
4.5	0.35	0.42	0.385	0.34	0.40	0.370	0.40
4.6	0.35	0.42	0.385	0.44	0.50	0.470	0.39

5 Conclusions

An innovative sheet metal joining process called rotated clinching was developed in this study. Rotated clinching involves two rotated heads with the same structure and size and a fixed die with a square flat bottom. The joining of metallic sheets can be realised through this method by rotating the rotated heads. Preliminary tests were conducted on 1.5-mm-thick Al1060 sheets to verify the feasibility of this process. Joints with different vertical reductions of the rotated heads were analysed by performing different mechanical tests, including lap shear tests in transverse and longitudinal directions, pull-out tests in the thickness direction, and joint failure modes. In addition, the geometrical parameters of the joint profile, such as Δt, Δs, and X_{min}, were measured under various vertical reductions. The main results are as follows:
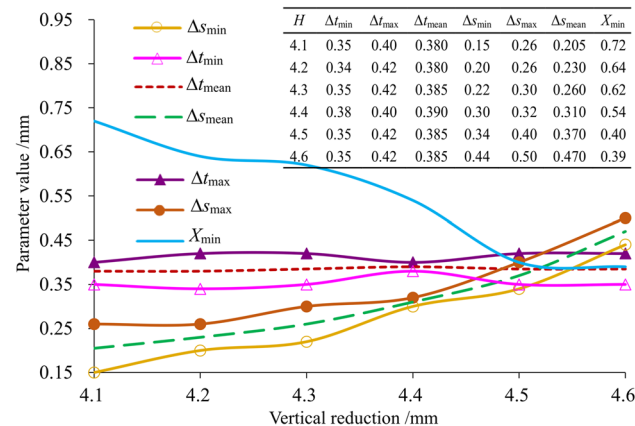
(1) The maximum shear strength in the transverse direction was 1090 N, the maximum shear strength in the longitudinal direction was 388 N, and the maximum pull-out strength in the thickness direction was 623 N, which are 40%, 14.4%, and 23%, respectively, of the corresponding values for Al1060. The mechanical test results of the joints in different directions showed that the shear strength in the transverse direction was the largest, at 2.3–3 times the shear strength in the longitudinal direction and 1.9–2.3 times the pull-out strength in the thickness direction.

(2) The rotated clinching process yielded high interlock by rotating a pair of rotated heads. With increasing reduction of the rotated heads, the interlock increased, bottom thickness decreased, and neck thickness of the

joint remained almost constant. When $H = 4.6$ mm, the maximum interlock was 0.5 mm.

(3) The failure modes of the joints were considerably affected by the force direction. Four types of failure modes of the joints were observed: full tearing, full unbuttoning, partial unbuttoning with tearing, and partial unbuttoning with shearing. Full tearing and partial unbuttoning with tearing were the main failure modes.

(4) The preliminary test results prove that two layers of 1.5-mm-thick Al1060 sheets can be successfully joined by a rotated clinching process with a flat-bottomed fixed die.

Although the static joining strength of a single point joint created by rotated clinching may be lower than that of a traditional round joint, this work will enable more effective sheet multipoint joining in various manufacturing fields. In future research, the factors influencing the asymmetries and joining strength will be investigated, and the joining strength of the joints will be further improved by optimising the tool structures and process parameters.

Declarations

References

1. Santos M, Machado A, Sales W, Barrozo M, Ezugwu E (2016) Machining of aluminum alloys: a review. Int J Adv Manuf Technol 86:3067–3080. https://doi.org/10.1007/s00170-016-8431-9
2. Briskham P, Blundell N, Han L, Hewitt R, Boomer D (2006) Comparison of self-pierce riveting, resistance spot welding and spot friction joining for aluminium automotive sheet. SAE Technical Papers 20–34. https://doi.org/10.4271/2006-01-0774
3. Varis J (2006) Economics of clinched joint compared to riveted joint and example of applying calculations to a volume product. J Mater Process Technol 172:130–138. https://doi.org/10.1016/j.jmatprotec.2005.09.009
4. Abe Y, Taromaru K, Kato T, Mori K (2011) Improvement of join-ability in mechanical clinching of sheets using step punch. Institute of Metal Forming. Special Edition: 10th International Conference on Technology of Plasticity, Aachen, Germany, 667–672
5. Hamel V, Roelandt JM, Gacel JN, Schmit F (2000) Finite element modeling of clinch forming with automatic remeshing. Comput Struct 77:185–200. https://doi.org/10.1016/s0045-7949(99)00207-2
6. Paulaa AA, Aguilarb M-T-P, Pertence A-E-M, Cetlin P-R (2007) Finite element simulations of the clinch joining of metallic sheets. J Mater Process Technol 182:352–357. https://doi.org/10.1016/j.jmatprotec.2006.08.014
7. Oudjene M, Ben-Ayed L (2008) On the parametrical study of clinch joining of metallic sheets using the Taguchi method. Eng Struct 30:1782–1788. https://doi.org/10.1016/j.engstruct.2007.10.017
8. Lee CJ, Kim JY, Lee SK, Ko DC, Kim BM (2010) Parametric study on mechanical clinching process for joining aluminum alloy and high-strength steel sheets. J Mech Sci Technol 24(1):123–126. https://doi.org/10.1007/s12206-009-1118-5
9. Mucha J (2011) The analysis of lock forming mechanism in the clinching joint. Mater Des 32:4943–4954. https://doi.org/10.1016/j.matdes.2011.05.045
10. Kim JY, Lee CJ, Lee SK, Ko DC, Kim BM (2009) Effect of shape parameters of tool on improvement of joining strength in clinching. Trans Mater Proces 18:392–400. https://doi.org/10.5228/KSPP.2009.18.5.392
11. Coppieters S, Zhang H, Xu F, Vandermeiren N, Breda A, Debruyne D (2017) Process-induced bottom defects in clinch forming: simulation and effect on the structural integrity of single shear lap specimens. Mater Des 130:336–348. https://doi.org/10.1016/j.matdes.2017.05.077
12. Brzezin´ski T, Ciccoli N, Dabrowski L, Sitarz A (2018) Mechanical clinching with dies for control of metal flow of ultra-high-strength steel and high-strength steel sheets. P I Mech Eng B-J Eng 232(4):644–649. https://doi.org/10.1177/0954405416683429
13. Abe Y, Mori K, Kato T (2012) Joining of high strength steel and aluminium alloy sheets by mechanical clinching with dies for control of metal flow. J Mater Process Technol 212:884–889. https://doi.org/10.1016/j.jmatprotec.2011.11.015
14. Lee CJ, Lee JM, Ryu HY, Lee KH, Kim BM, Ko DC (2014) Design of hole-clinching process for joining of dissimilar materials Al6061-T4 alloy with DP780 steel, hot-pressed 22MnB5 steel, and carbon fiber reinforced plastic. J Mater Process Technol 214:2169–2178. https://doi.org/10.1016/j.jmatprotec.2014.03.032
15. NeugebauerR KC, Dietrich S (2008) Advances in mechanical joining of magnesium. CIRP Ann Manuf Technol 57:283–286. https://doi.org/10.1016/j.cirp.2008.03.025
16. Gerstmann T, Awiszus B (2014) Recent development in flat-clinching. Comput Mater Sci 81:39–44. https://doi.org/10.1016/j.commatsci.2013.07.013
17. Atia MKS, Jain MK (2017) Die-less clinching process and joint strength of AA7075 aluminum joints. Thin-Walled Struct 120:421–431. https://doi.org/10.1016/j.tws.2017.06.021
18. Luder S, Hartel S, Binotsch C, Awiszus B (2014) Influence of the moisture content on flat-clinch connection of wood materials and aluminium. J Mater Process Technol 214:2069–2074. https://doi.org/10.1016/j.jmatprotec.2014.01.010
19. Han XL, Zhao SD, Chen C, Liu C, Xu F (2017) Optimization of geometrical design of clinching tools in flat-clinching. Proc IMechE C 231:4012–4021. https://doi.org/10.1177/0954406216660335

20. Chen C, Zhao S, Han X, Wang Y, Zhao X (2020) Investigation of the flat-clinching process for joining three-layer sheets on thin-walled structures. Thin-Walled Struct 157:107034. https://doi.org/10.1016/j.tws.2020.107034

21. He YL, Huang LJ (2013) An experimental research on quality and strength of aluminous joint by clinch joining technique applied mechanical and material. Appl Mech Mater 389:217. https://doi.org/10.4028/www.scientific.net/amm.389.217

22. Lambiase F, Di Ilio A (2013) Finite element analysis of material flow in mechanical clinching with extensible dies. J Mater Eng Perform 22:1629–1636. https://doi.org/10.1007/s11665-012-0451-5

23. Lambiase F, Di Ilio A (2014) An experimental study on clinched joints realized with different dies. Thin-Walled Struct 85:71–80. https://doi.org/10.1016/j.tws.2014.08.004

24. He X, Liu F, Xing B, Yang H, Wang Y, Gu F, Ball A (2014) Numerical and experimental investigations of extensible die clinching. Int J Adv Manuf Technol 74:1229–1236. https://doi.org/10.1007/s00170-014-6078-y

25. Han X, Zhao S, Liu C, Chen C, Xu F (2017) Optimization of geometrical design of clinching tools in clinching process with extensible dies. Proc IMechEC 231:3889–3897. https://doi.org/10.1177/0954406216660336

26. He X, Zhang Y, Xing B, Gu F, Ball A (2015) Mechanical properties of extensible die clinched joints in titanium sheet materials. Mater Des 71:26–35. https://doi.org/10.1016/j.matdes.2015.01.005

27. Witkowski W (2015) The shear strength of the round clinching joints formed by using extensible dies. Adv Sci Technol Res J 9(26):72–76. https://doi.org/10.12913/22998624/2367

28. Mucha J (2011) The analysis of rectangular clinching joint in the shearing test. Maint Reliab 3:45–50

29. Varis JP (2003) The suitability of clinching as a joining method for high-strength structural steel. J Mater Process Technol 132:242–249. https://doi.org/10.1016/s0924-0136(02)00933-0

30. Zhao L, He XC, Lu Y (2014) Research of mechanical behavior for rounded and rectangular clinched joint. Adv Mater Res 1035:144–148. https://doi.org/10.4028/www.scientific.net/amr.1035.144

31. Lambiase F (2015) Mechanical behaviour of polymer–metal hybrid joints produced by clinching using different tools. Mater Des 87:606–618. https://doi.org/10.1016/j.matdes.2015.08.037